



Returning low C/N crop straw to the paddy field can achieve the dual benefits of reduced methane emissions and enhanced yield stability

Chuanhai Shu^a, Binbin Liu^a, Yu Li^c, Qiqi Chen^a, Leilei Li^a, Yuanqing Shi^a, Hongkun Xie^a, Zhonglin Wang^a, Qin Liao^a, Qingyue Cheng^a, Feijie Li^d, Na Li^b, Zongkui Chen^{a,b}, Yongjian Sun^{a,b}, Zhiyuan Yang^{a,b,*}, Jun Ma^{a,b,*}

^a Rice Research Institute, Sichuan Agricultural University, Chengdu 611130, China

^b Crop Ecophysiology and Cultivation Key Laboratory of Sichuan Province, Chengdu 611130, China

^c Chuanzhong Seed Industry, Chengdu 611532, China

^d Rongxian Bureau of Agriculture and Rural Affairs, Zigong 643100, China



ARTICLE INFO

Keywords:

Rice

Upland-paddy rotation systems

Methane

ABSTRACT

The combination of upland-paddy rotation and straw returning is a common practice in China's subtropical regions. However, the effect and mechanisms of returning the upland crop residues to the paddy field on methane (CH_4) emissions during the rice (*Oryza sativa* L.) season under different upland-paddy rotation systems remain scarce. To this end, a two-year field experiment (2023–2024) compared five of the most popular rotation systems: wheat-rice, rapeseed-rice, green vegetable-rice, *Vicia villosa* var.-rice, and fallow-rice in the Sichuan Basin. CH_4 emissions, rice yields, greenhouse gas intensity, and soil methanogenic and methanotrophic gene abundances were measured. Dry-season crops received distinct fertilizer inputs, while rice-season management remained uniform. The results showed that: wheat-rice had the highest abundance of the methanogenic gene (5.00×10^7 and 2.27×10^7 copies g^{-1} soil in 2023 and 2024, respectively) during the rice growth period, resulting from high carbon-to-nitrogen ratio straw inputs (43.91), which enhanced methanogen activity, leading to the largest cumulative CH_4 emissions (683.41 and 238.65 kg hm^{-2}) and higher rice yields (7741.83 and 8231.04 kg hm^{-2}). Therefore, the greenhouse gas intensity of wheat-rice (2.22 and 0.74 $\text{kg CO}_2\text{-eq kg}^{-1}$ grain yield) was significantly higher than that of other systems. In contrast, the *Vicia villosa* var.-rice (147.56 and 39.55 kg hm^{-2}) rotation with low carbon-to-nitrogen ratio straw (11.28) reduced cumulative CH_4 emissions compared to wheat-rice through balancing methanogenic and methanotrophic gene abundances (ratio 0.61–1.19), while maintaining stable yields (7668.22–8614.37 kg hm^{-2}). The yield of the *Vicia villosa* var.-rice rotation system was not significantly different from green vegetable-rice (8117.98 and 9203.85 kg hm^{-2}) and was higher than that of the other systems. Notably, *Vicia villosa* var.-rice achieved the lowest greenhouse gas intensity (0.48–0.12 $\text{kg CO}_2\text{-eq kg}^{-1}$) by synergistically optimizing carbon-nitrogen dynamics and soil organic carbon sequestration. The above results indicate that the *Vicia villosa* var.-rice rotation system exhibits superior performance in terms of stable yield and emission reduction. This study highlights that the straw carbon-to-nitrogen ratio plays a pivotal role in regulating methane metabolism and maintaining carbon-nitrogen balance, thereby presenting a climate-smart strategy for rice cultivation. It provides a robust scientific foundation for optimizing crop rotation systems and contributes to mitigating agricultural greenhouse gas emissions.

1. Introduction

Climate change has become a core issue in global governance. The Sixth Assessment Report (AR6) of the Intergovernmental Panel on Climate Change (IPCC) indicates that the global surface temperature has

increased by 1.09°C relative to pre-industrial levels (IPCC, 2023). This warming trend has a profound impact on the global ecological environment. Methane (CH_4), as a more potent greenhouse gas (GHG) than carbon dioxide (CO_2), plays an essential role in global warming. Its 100-year warming potential is 28 times that of CO_2 (IPCC, 2014a),

* Corresponding authors at: Rice Research Institute, Sichuan Agricultural University, Chengdu 611130, China.

E-mail addresses: 14236@sicau.edu.cn (Z. Yang), majunp2002@163.com (J. Ma).

accounting for about 16 % of the radiative intensity of GHG (WMO, 2020), significantly influencing global climate warming and the destruction of the ecological environment. China is the world's largest producer and consumer of rice (*Oryza sativa* L.), accounting for 18.5 % and 31 % of the world's rice fields and output, respectively (IPCC et al., 2014b). The rice fields in China account for 27 % of the country's total cultivated land area (Zhu et al., 2022). While rice plays a crucial role in ensuring China's food self-sufficiency, it is also a significant contributor to agricultural GHG emissions. Previous studies have shown that in 2021, the CH₄ emissions from rice paddies in China were approximately 5.29 Tg, accounting for 21.61 % of the total global CH₄ emissions from rice cultivation (Peng et al., 2021). Therefore, balancing land output and GHG emissions has become an important research direction in China's agricultural production, especially rice production (Zhou et al., 2016).

Due to the large population and limited land, in order to increase output, China's rice production methods have been optimized over thousands of years and have gradually developed various models, including double-cropping rice, ratoon rice, and upland-paddy rotation systems such as wheat (*Triticum aestivum* L.)-rice (RW), rapeseed (*Brassica campestris* L.)-rice (RR), and green vegetable (*Brassica juncea* var.)-rice (RG) (Zheng et al., 2016; Wang et al., 2018). Most of these models rely on intensive land cultivation, maximizing the utilization of light and heat resources. As awareness of soil protection grows, single-season systems such as the winter fallow field-rice system and the green manure-rice system are gradually emerging. Each production system has its characteristics for achieving soil enrichment or high yield (Wu et al., 2020b; Fang et al., 2023). The rice-wheat rotation system is the predominant cropping system in East Asia, with approximately 60 % of rice paddies in southeastern China adopting this practice (Wu et al., 2021). However, because the system involves irrigated rice fields and dryland wheat fields, assessing GHG emissions from the entire rotation system remains challenging (Hou et al., 2016). Different straw-returning treatments significantly impacted seasonal CH₄ emissions and increased the annual soil organic carbon (SOC) sequestration rate in the topsoil (Wang et al., 2019), thereby improving soil structure and potentially enhancing long-term soil health (Kan et al., 2023). Long-term straw returning to the paddy field can also help increase rice yields and reduce CH₄ emissions (Yang et al., 2022). In a 32-year wheat straw return experiment, the long-term incorporation of straw significantly enhanced soil organic matter and fertility, stimulated root growth, and improved soil aeration. These changes collectively increased the potential for methane oxidation and promoted the abundance of methanotrophs (Yang et al., 2022), demonstrating the long-term effect of straw management on regulating soil methane metabolism.

Different crop straw returns release varying amounts of nitrogen during decomposition, primarily determined by the straw's carbon-to-nitrogen (C/N) ratio (Chivenge et al., 2011). Straw from crops such as wheat and rapeseed are characterized by low nitrogen content and high cellulose levels, leading to elevated C/N ratios. This condition restricts nitrogen mineralization and has a detrimental impact on crop yield (Yanni et al., 2011). In contrast, returning low C/N straw, which is rich in nitrogen, increases microbial activity and accelerates straw decomposition (Paul, 2015). Comparing the RW rotation with the RR rotation, the RR rotation has higher nitrous oxide (N₂O) emissions (Xu et al., 2023). Conversely, the CH₄ emission from RR rotation is higher, which is related to the lower SOC content in the early stage of wheat returning and the higher oxygen content in the soil during the dry-wet alternating irrigation of rapeseed, suppressing CH₄ emission (Jiang et al., 2022). Therefore, potential strategies to mitigate CH₄ emissions include altering the types of dryland crops and implementing alternate wet-dry irrigation techniques during the rice-growing season. The impact of non-rice crop planting mode on GHG emissions in double-rice areas also varies. For example, planting rapeseed can reduce GHG emissions (Tang et al., 2015). However, nitrogen fertilizer application during the rapeseed season increases CH₄ emissions during the rice seedling stage. Green manure crops play an important role in reducing fertilizer

application and improving soil fertility. CH₄ emissions are significantly positively correlated with dissolved organic carbon as well as the biomass and C/N ratio of incorporated green manure plant materials (Raheema et al., 2019). Green manure is mainly planted on the soil and plowed into the soil after maturity (Tang et al., 2015). Its role in reducing crop nitrogen requirements and maintaining yields has been well documented (Salahin et al., 2013). *Vicia villosa* var. can maintain rice yield while minimizing CH₄ emissions in Korean monocropping systems (Kim et al., 2013). Similar reports from South China showed that *Vicia villosa* var. could minimize CH₄ emissions compared with ryegrass (Tang et al., 2015). *Vicia villosa* var.-rice (RV) rotation significantly reduced CH₄ emissions compared with rice monoculture (Zhang et al., 2019), but it was higher than that in wheat-rice rotation, which indicates that the effects of different winter cover crops on CH₄ emissions from rice fields vary from place to place (Zhang et al., 2013). Other studies have also confirmed that covering different crops in winter can change CH₄ emissions from rice fields (Cha-un et al., 2017).

From a microbial perspective, methane emissions in paddy fields are primarily driven by methanogens, which utilize substrates such as acetate, hydrogen, and CO₂ to produce CH₄. In contrast, methanotrophs consume CH₄ under aerobic conditions through the action of the *pmoA* gene. Previous studies have shown that different types of crop straw and their C/N ratios influence the relative abundance of these two functional groups, as represented by the *mcrA/pmoA* gene ratio, thereby significantly affecting net CH₄ fluxes in paddy soils. Under high C/N treatments, such as incorporating wheat straw, this ratio increases, leading to elevated methane emissions. Conversely, incorporation of low C/N green manures such as *Vicia villosa* var. enhances *pmoA* expression and suppresses *mcrA*, thereby reducing CH₄ emissions (Yang et al., 2022; Zhou et al., 2024a). Although this mechanism has been preliminarily identified, systematic investigations into its dynamics across diverse upland-paddy rotation systems remain scarce.

Most existing studies focus on greenhouse gas emissions under single rotation systems (e.g., wheat-rice or rapeseed-rice). However, there is a limited mechanistic understanding of how the C/N ratio of preceding crop residues regulates CH₄ emissions via microbial processes in diversified upland-paddy rotation systems. Specifically, the influence of the straw C/N ratio on CH₄ emissions through alterations in the relative abundance of methanogens (indicated by the *mcrA* gene) and methane-oxidizing bacteria (indicated by the *pmoA* gene), as expressed by the *mcrA/pmoA* ratio, remain unclear. In this study, the following hypotheses are proposed: (1) Returning high C/N residues will increase the *mcrA/pmoA* ratio and thereby enhance CH₄ emissions; (2) Returning low C/N residues will reduce CH₄ emissions by suppressing the *mcrA/pmoA* ratio while ensuring sufficient nitrogen release to maintain rice yield; (3) The straw C/N ratio is positively correlated with greenhouse gas intensity (GHGI), and low C/N systems can achieve both emission reduction and productivity gains. To test these hypotheses, a two-year field experiment was conducted to explore the regulatory mechanisms of different straw C/N inputs on CH₄ emissions during the rice-growing season. The findings aim to provide a scientific basis for optimizing rotation strategies and developing C/N-based low-carbon management practices in paddy fields.

2. Materials and methods

2.1. Experimental location

This experiment was conducted at the Experimental Farm of the Rice Research Institute of Sichuan Agricultural University, Wenjiang District, Chengdu City, Sichuan Province (30°43' N, 103°47' E). As shown in Fig. 1c, consecutive annual tests were conducted during 2022–2023 and 2023–2024. The temperature and rainfall data for the test area over these two years are presented in Fig. 1a, b. The test site is a typical subtropical humid monsoon climate. The soil of the test field is sandy loam soil, and the physical and chemical properties of the basic soil are

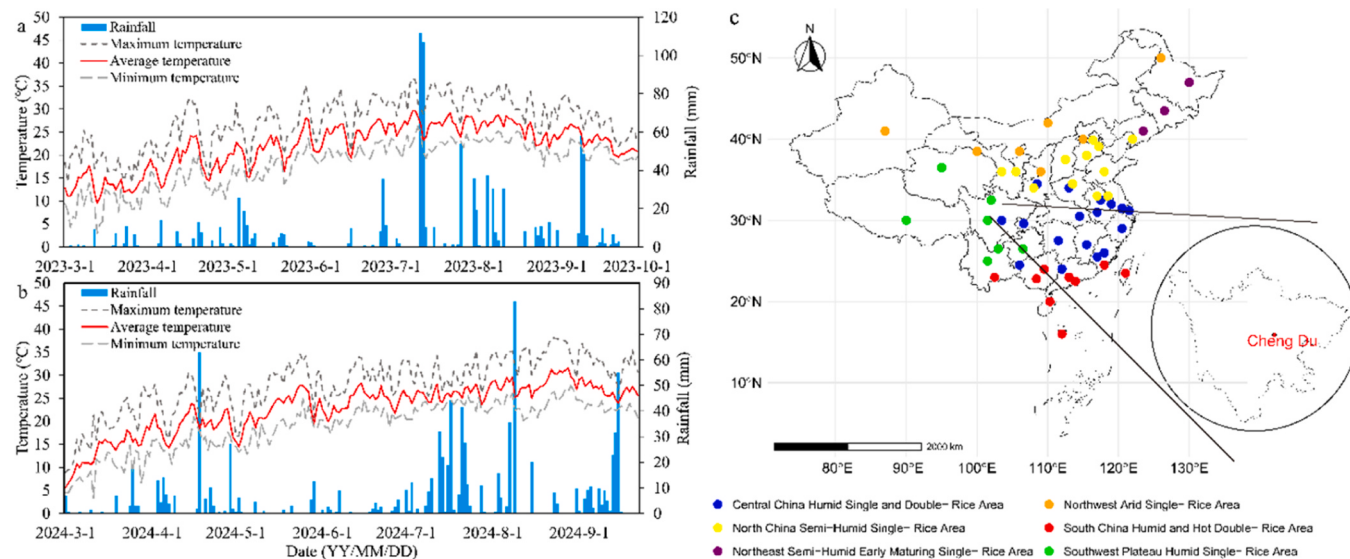


Fig. 1. Location of the experimental site.

shown in Table 1.

2.2. Experimental design

The experiment utilized a single-factor randomized block design, incorporating the five most popular rice rotation treatments: RW, RR, RG, green manure-rice (where the green manure was primarily *Vicia villosa* var. grown locally-RV), and RF. Each treatment was replicated three times, with each plot measuring 30 m², resulting in a total of 15 plots. Implementation details of various crop rotation systems (Table 2, Fig. 2) are optimized based on previous research and local production practices (Song et al., 2023; Xie et al., 2023). The straw and its attachments left after the previous crop are plowed back into the field after the start of the rice-growing season, with wheat and rapeseed straw returned at a length of 10 cm and green vegetable litter and *Vicia villosa* var. directly incorporated. All residues were incorporated into the soil at a depth of 0–20 cm. The application times for basal fertilizer, tillering fertilizer, flower-promoting fertilizer, and flower-retaining fertilizer in rice cultivation are as follows: basal fertilizer is applied 1 day before transplanting; tillering fertilizer is applied 7 days after transplanting; flower-promoting fertilizer is applied when the fourth leaf from the top emerges; and flower-retaining fertilizer is applied when the second leaf from the top emerges. The nitrogen, phosphorus, and potassium fertilizers utilized in the experiment were urea (containing 46 % N), superphosphate (containing 12 % P₂O₅), and potassium chloride (containing 60 % K₂O). During the rice-growing season, both the fertilization practices and field management were consistent. The experimental fields are controlled for diseases, insects, and weeds in the same way as large-scale production fields.

2.3. Sample collection and determination

2.3.1. Soil sample collection and analysis

Soil samples from the farmland were collected at the jointing, full heading, and maturity stages of rice. Sampling was conducted between rice rows using a cylindrical sampler with a diameter of 5 cm at a depth of 0–20 cm. Five samples were collected from each period, thoroughly mixed in equal proportions, and subsequently stored in self-sealing bags. Upon transportation to the laboratory, the samples were air-dried naturally under cool and dry conditions to prepare for subsequent analysis of soil physical and chemical properties. At the same time, 0–20 cm rhizosphere soil samples were collected near rice roots at 5 points and stored in sterile self-sealing bags to determine soil

microorganisms.

SOC was determined using the potassium dichromate volumetric method-dilution heat method. A 0.5 g air-dried soil sample passed through a 100-mesh sieve and was weighed and placed in a 500 ml conical flask. Then, 10 ml of 1 mol L⁻¹ (1/6 K₂Cr₂O₇) solution was added and mixed well. After that, 20 ml of concentrated H₂SO₄ was added. Once the reagent and soil had fully reacted, the flask was placed on an asbestos board for 30 min. The mixture was then diluted with water to 250 ml, and 3–4 drops of o-phenanthroline indicator were added. Finally, titration was performed using 0.5 mol L⁻¹ FeSO₄ solution. Soil NO₃-N was extracted using 2 mol L⁻¹ of KCl solution and analyzed using a spectrophotometer (Multiskan Sky 1530, Thermo Scientific, Singapore).

2.3.2. Gas sample collection and determination

CH₄ and N₂O emissions were measured by static box-gas chromatography (Yuesi and Yinghong, 2003). The gas sampling box consists of a base and a top enclosure. The box body is fabricated from rigid polyvinyl chloride plastic, forming a sealed hollow rectangular prism with dimensions of 0.34 m in length, 0.34 m in width, and 1.2 m in height. To maintain the stability of the internal gas temperature, the exterior of the box is insulated with thermal film and covered with aluminum foil. A sampling port is located on the top of the box, which is connected to a three-way valve for gas collection. Additionally, a thermosensitive electronic thermometer is installed to provide real-time monitoring of the internal temperature. Four 12 V small square fans are installed on the top of the box and connected to a portable power supply to fully mix the gas in the box. The static box has a base with dimensions of length × width × height = 0.34 m × 0.34 m × 0.15 m. A groove, measuring 5 cm in depth and 5 cm in width, is located on the top of the base. The inner dimensions of the groove are slightly smaller than the inner diameter of the gas sampling box, allowing for easy embedding of the box into the groove. Additionally, the blank portion of the groove is sealed with water to maintain the closed state of the sampling box. The gas sampling time was between 8:30 a.m. and 11:30 a.m. Before gas collection, 12 ml headspace glass bottles (Labco Exetainer, Labco Limited, UK) were subjected to vacuum treatment. At 0, 10, 20, and 30 min after the box was sealed, 12 ml of the mixed gas inside the box was collected with a syringe into the vacuum glass bottles and returned to the laboratory for determination. The measurement cycle encompassed the entire period from rice transplantation to harvest. Gas samples were collected every 3 days following nitrogen fertilizer application and every 7 days during other periods.

Table 1
Basic soil physical and chemical properties during the rice-growing season.

Year	Crop Rotation	Organic matter (g kg^{-1})	Total C (g kg^{-1})	Total N (g kg^{-1})	Alkali hydrolyzable N (mg kg^{-1})	Available P (mg kg^{-1})	Available K (mg kg^{-1})	pH	BD (g cm^{-3})
2023	RW	20.47 b	14.36 a	1.38 ab	101.03 a	29.86 b	58.3 c	5.43 b	1.27 a
	RR	18.63 c	14.17 a	1.35 ab	102.1 a	17.96 c	96.84 b	5.53 b	1.36 a
	RG	22.16 a	14.25 a	1.41 a	118.12 a	41.24 a	154.86 a	5.11 c	1.24 a
	RV	22.09 a	13.49 a	1.34 ab	100.9 a	34.78 ab	35.75 cd	5.38 b	1.28 a
	RF	17.86 d	12.53 b	1.31 b	100.33 a	41.55 a	27.78 d	5.75 a	1.27 a
	Average	20.24	13.76	1.36	104.5	33.08	74.71	5.44	1.29
2024	RW	21.43 a	13.87 a	1.36 a	97.85 b	26.74 b	156.49 a	5.55 a	1.22 a
	RR	21.23 a	14.14 a	1.39 a	119.59 a	14.77 c	139.08 a	5.54 a	1.18 a
	RG	20.33 b	13.84 a	1.39 a	97.44 b	43.41 a	157.27 a	5.55 a	1.1 a
	RV	19.95 b	13.96 a	1.35 a	96.08 b	21.42 bc	167.06 a	5.52 a	1.31 a
	RF	20.44 b	12.87 b	1.27 b	99.17 b	46.8 a	49.03 b	5.74 a	1.29 a
	Average	20.67	13.74	1.35	102.03	30.63	133.78	5.58	1.22
F-value	Y	**	**	*	ns	ns	ns	ns	ns
	C	**	**	ns	ns	ns	ns	**	**
	Y*C	**	**	ns	ns	ns	ns	*	*

Notes: RW: wheat-rice; RR: rapeseed-rice; RG: green vegetables-rice; RV: *Vicia villosa* var.-rice.; RF: winter fallow field -rice; BD: bulk density. Different lowercase letters within the same column indicate significant differences at the 0.05 level (LSD test) between different crop rotation systems.

The concentrations of CH_4 and N_2O were determined by gas chromatography (Clarus 590, PerkinElmer), with a single-valve single-column injection and separation gas path for CH_4 , an FID (hydrogen flame ionization detector), a detection temperature of 380 °C, and a column temperature of 55 °C. N_2O adopted double-valve double-column automatic sampling, backflush, separation, and switching gas path. The detector was an ECD (electron capture detector) with a detector temperature of 300 °C, a column temperature of 55 °C, and a carrier gas of 99.999 % high-purity N_2 . The flow rate was 30 ml min⁻¹, and the emission rate was obtained by linear regression of four gas concentrations. The emission flux of CH_4 and N_2O was calculated according to the following equation:

$$F = \rho \times H \times \frac{\Delta_c}{\Delta_t} \times \frac{273}{273 + T} \quad (1)$$

where F is the gas emission flux ($\text{mg m}^{-2} \text{h}^{-1}$); ρ is the gas density under standard conditions ($\text{CH}_4 = 0.714 \text{ kg m}^{-3}$, $\text{N}_2\text{O} = 1.964 \text{ kg m}^{-3}$); H is the cylinder height (m); Δ_c/Δ_t is the rate of change of gas concentration in the sampling box with time ($\text{ml m}^{-3} \text{h}^{-1}$); T is the average temperature in the sampling box (°C); 273 is the constant of the gas state equation.

During the collection of gas samples, a portable thermometer (TP330, Sanyin Trading) was employed to monitor the temperature within the sampling chamber. Additionally, a redox potential meter (TR-901, Lei-ci) was utilized to measure both the soil redox potential and soil temperature. Furthermore, a ruler was applied to determine the water depth on the field surface during paddy field flooding.

The cumulative CH_4 and N_2O emissions are calculated as follows:

$$C = \sum_i^n (F_{i+1} + F_i) / 2 \times (d_{i+1} - d_i) \times 24 \quad (2)$$

where C is the cumulative emission of CH_4 and N_2O (kg hm^{-2}), F_i and F_{i+1} are the gas emission fluxes in two consecutive adjacent sampling periods; d_{i+1} and d_i represent the dates of the i and $i+1$ sampling, respectively.

The combined emissions of CH_4 and N_2O are converted into CO_2 equivalents according to the greenhouse effect. The global warming potential (GWP) is calculated as follows:

$$\text{GWP} = \text{CH}_4 \times 28 + \text{N}_2\text{O} \times 265 \quad (3)$$

where GWP is the global warming potential ($\text{kg CO}_2\text{-eq hm}^{-2}$).

GHGI refers to the comprehensive greenhouse effect CO_2 equivalent per unit of output ($\text{kg CO}_2\text{-eq kg}^{-1}$ grain yield), which can be calculated as follows:

$$\text{GHGI} = \text{GWP}/Y \quad (4)$$

where GHGI is greenhouse gas emission intensity ($\text{kg CO}_2\text{-eq kg}^{-1}$ grain yield); Y is rice grain yield (kg hm^{-2}).

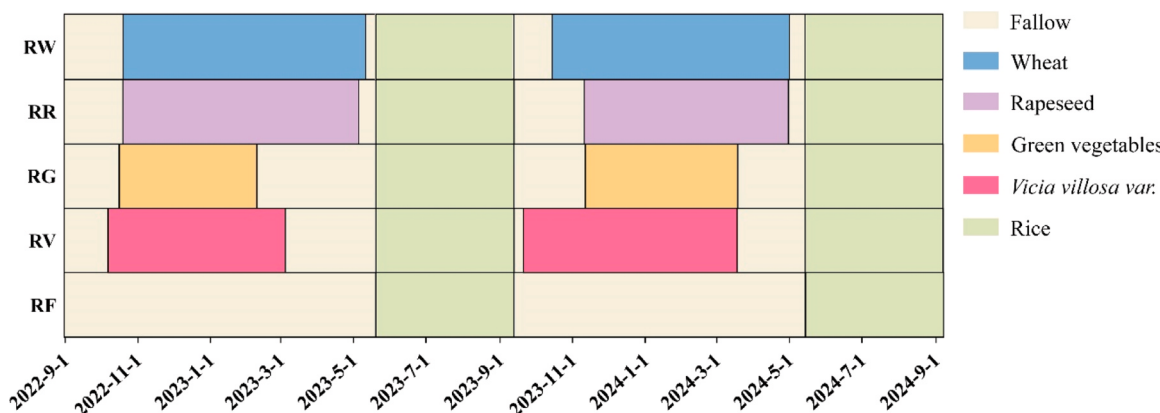
2.3.3. Fluorescence quantitative PCR of functional genes *mcrA* and *pmoA*

The gene abundance of soil methanogens and methanotrophs was determined by real-time fluorescence absolute quantitative polymerase chain reaction (RT-qPCR) technology, with the functional gene *mcrA* (encoding the methyl coenzyme M reductase subunit) and the *pmoA* gene (encoding the CH_4 monooxygenase subunit) as marker genes. First, 0.25–0.5 g of fresh soil was weighed, and the total soil DNA was extracted using the Bio-Base-XPure Soil DNA Extraction Kit (Beijing Aidlab Biotechnologies Co., Ltd.). The size of the extracted DNA fragments was detected by 10 g L⁻¹ agarose gel electrophoresis, and the DNA concentration and quality were determined using an ultra-micro nucleic acid protein analyzer (ScanDrop 100). Primers for the *mcrA* gene of methanogens and the *pmoA* gene of methanotrophs were designed for real-time fluorescence quantitative PCR analysis. The reaction system included 5 μL 2X ChamQ SYBR ® Color qPCR Master Mix, 0.4 μL each of upstream and downstream primers, 0.2 μL 50 X ROX

Table 2

Different crop fertilization rates and the ratio of base fertilizer to top dressing.

Crop rotation systems	Crop	Variety	Seeding method	Fertilizer dosage (kg hm ⁻²)			Base fertilizer topdressing ratio
				N	P ₂ O ₅	K ₂ O	
Previous crop	wheat	<i>ShuMai 1963</i>	direct seeding	180	90	90	Base fertilizer: jointing fertilizer = 5:5, phosphate fertilizer and potassium fertilizer are applied as base fertilizer at one time
	rapeseed	<i>YouYan 2013</i>	seedling transplantation	180	90	180	Base fertilizer: bolting fertilizer = 7:3. Phosphate and potash fertilizers are applied entirely as base fertilizers.
	green vegetables	<i>Brassica juncea</i> var. <i>capitata</i> 'Te Xuan Dapingpu'	seedling transplantation	240	120	188	base fertilizer: top dressing = 5:5. Phosphate and potash fertilizers are applied entirely as base fertilizers.
	green manure	<i>Vicia villosa</i> var.	direct seeding				
The following crop	rice	<i>ChuanKang You 2115</i>	seedling transplantation	150	75	150	Base fertilizer: tillering fertilizer: promoting flower fertilizer: flower fertilizer = 3:3:3:2, phosphate fertilizer and potassium fertilizer are applied entirely as base fertilizers.

**Fig. 2.** Planting and harvesting times of crops under different crop rotation systems. RW: wheat-rice; RR: rapeseed-rice; RG: green vegetables-rice; RV: *Vicia villosa* var.-rice.; RF: winter fallow field -rice.

Reference Dye 1, 1 µL DNA template, and 3 µL sterile distilled water. The reaction system was added to a 96-well plate, and each sample was repeated three times. RT-qPCR analysis was performed using a fluorescent quantitative PCR instrument (ABI7300, Applied Biosystems, USA). The PCR reaction conditions were: Pre-denaturation at 95 °C for 5 min, denaturation at 95 °C for 30 s, annealing at 58 °C for 30 s, and extension at 72 °C for 1 min. The plasmid containing *mcrA* and *pmoA* genes (pMD18-T) was used to plot the standard curve, and the plasmid was diluted 10 times before use. The amplification efficiency of *mcrA* and *pmoA* genes reached 109.10 % and 108.64 %, respectively, and the R² values were 0.996 and 0.997, respectively. The primers used for quantitative PCR analysis of each gene are shown in Table 3.

2.3.4. Determination of biological yield and economic yield

During the maturity period of rice and wheat, the outer rows of each plot were removed prior to manual harvesting. Grain yield was calculated based on the actual harvested samples. The water content of rice grains was 13.5 %, while that of wheat grains was 12.5 % (Ding et al., 2022).

The rapeseed yield in each plot was calculated at the harvest stage, and the water content of the seed was 9 % (Deng et al., 2024).

Green vegetables were harvested when the pods fully turned yellow and dried. The yield was determined based on the actual harvest, excluding the border rows in each plot (Wu et al., 2020a).

When *Vicia villosa* var. reached the peak flowering stage, the aboveground biomass of each plot was measured, and the yield was estimated based on actual harvest data.

In each plot, 200 g of wheat straw, rapeseed straw, green vegetables, and *Vicia villosa* var. were collected and placed in 80-mesh nylon bags. These samples were then subjected to blanching at 105 °C for 30 min in an electric constant temperature air drying oven (Jing Hong Experimental Equipment Co., Ltd.; model DHG-9240A). Following this, the samples were dried at 70 °C until they reached a constant weight. Subsequently, the dried samples were ground using a cyclone mill (Zhejiang Topu Yunnong Technology Co., Ltd.; model FS-II) and sieved through a 100-mesh screen to prepare them for the determination of carbon (C) and nitrogen (N) content (Dong et al., 2023).

2.3.5. Statistical analysis

Statistical analyses were performed using SPSS 22.0 for Windows (SPSS Inc., USA). Plotting was performed using OriginPro 2023b (OriginLab Inc., USA). One-way analysis of variance (ANOVA) was

Table 3

Real-time quantitative PCR primers.

Target gene	Primer	Primer	Reference
<i>mcrA</i>	MLfF MLrR	GGTGGGTGMGGATTCACACARTAYGCWACAGC TTCAATTGCRTAGTTWGGRTAGTT	(Luton et al., 2002)
<i>pmoA</i>	A189F Mb661R	GGNGACTGGGACTTCTGG CCGGMGCAACGTCYTTACC	(Tuomivirta et al., 2009)

employed to examine the relationships between various parameters and indicators across different crop rotation systems. The least significant difference (LSD) method (including student's *t*-test and F-test) was used to analyze and compare whether there were significant differences among the parameters of this study. Pearson correlation analysis was conducted to examine the relationships among all relevant parameters in this study (* $p < 0.05$, ** $p < 0.01$, *** $p < 0.001$).

The error bar in the figure of each chapter of this study represents the standard deviation; different lowercase letters in the figure indicate that there are significant differences in the data between different treatments in the same experimental site at the 0.05 level; different uppercase letters in the figure indicate that there are significant differences in the data between the same treatments in different experimental sites at the 0.01 level.

3. Results

3.1. Returning straw

There were significant differences in dry matter mass, carbon, and nitrogen contents of the previous crop straw returned to the paddy field. In terms of straw dry matter, RV (25,403.25–36,157.45 kg hm⁻²) was the highest, followed by RW (5561.55–7545.31 kg hm⁻²) and RR (3775.28–6031.38 kg hm⁻²), and RG (1386.67–1586.50 kg hm⁻²) was the lowest (Fig. 3a). The total carbon input of straw varies greatly with the type of previous crop, with higher carbon inputs for RV, RW, and RR, and lower carbon inputs for RG (Fig. 3b). The total nitrogen input of straw was the highest in RV, and there was no significant difference among RW, RR, and RG (Fig. 3c). The carbon-nitrogen ratios of the previous straw exhibited significant variation, with higher values observed in RW (43.91) and RR (43.86), and lower values in RG (8.65) and RV (11.28) (Fig. 3d).

The differences between years were mainly reflected in straw dry

matter mass, total C content, total N content, and C/N ratio. Compared to 2023, in the 2024 experiments, the dry matter mass of RV and RG increased by 42.33 % and 14.41 %, respectively, whereas that of RW and RR decreased by 37.40 % and 26.29 %, respectively. In terms of total carbon content, RV and RG increased by 46.99 % and 13.97 %, respectively, while RW and RR decreased by 23.26 % and 33.67 %, respectively. The total nitrogen content changed significantly, with RV and RG increasing by 22.34 % and 36.78 %, respectively, and RW and RR decreasing by 22.38 % and 31.88 %, respectively. There was no significant difference in the C/N ratio between the two years.

3.2. CH₄ emissions

The two-year CH₄ emission fluxes were different under different crop rotation systems. In 2023, CH₄ emissions from different rotation systems peaked when rice turned green to the jointing stage (7–33 days) and the heading stage (66–80 days). In 2024, CH₄ emissions peaked during the tillering stage (4–11 days) and the heading stage (63–78 days). The differences between the peak and valley values of CH₄ emission fluxes in RW and RR were 82.07 and 70.71 mg m⁻² h⁻¹, respectively. Additionally, the average CH₄ emission fluxes in RW and RR were 2.8 and 1.9 times higher than in RF, respectively. The peak-to-valley difference of CH₄ emission flux in RG and RV was 56.29 mg m⁻² h⁻¹ and 22.02 mg m⁻² h⁻¹, respectively. The average CH₄ emission flux of RG was not significantly different from that of RF, and RV was 39.39 % lower than that of RF (Fig. 4a-b). In 2024, the CH₄ emission flux of different rotation systems was higher 15 days after rice transplanting and at the heading stage. The CH₄ emission trends of each treatment were similar to those in 2023, but the emission flux was significantly reduced by 75.40 %–93.45 %, possibly related to the significant reduction in precipitation (Fig. 4c-d). There was a significant interaction effect between the year and treatment of total CH₄ emissions. In 2023, RW (683.41 kg hm⁻²) and RR (459.17 kg hm⁻²) were 1.8 times and 0.88

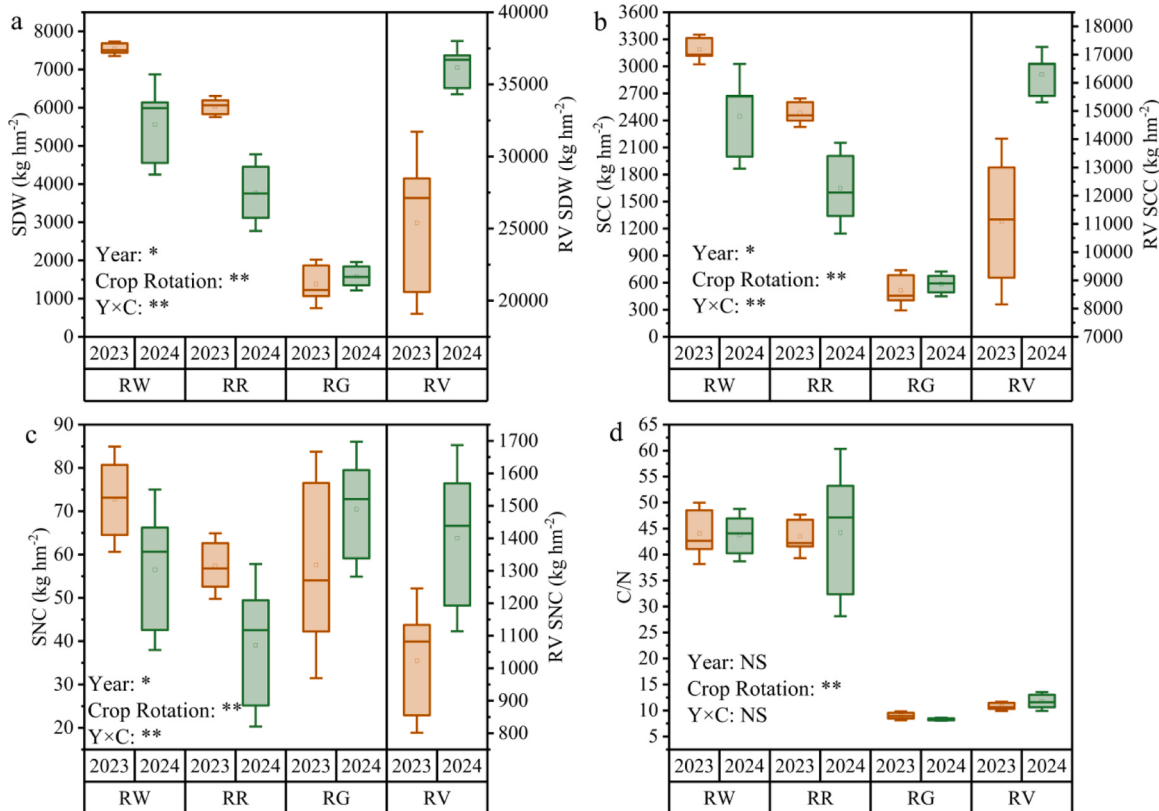


Fig. 3. Yield and carbon and nitrogen content of returning straw. RW: wheat-rice; RR: rapeseed-rice; RG: green vegetables-rice; RV: *Vicia villosa* var.-rice.; RF: winter fallow field-rice; SDW: Straw dry weight; Straw C cumulative; SNC: Straw N cumulative. The error bars in the figure represent the standard deviation (STDEV).

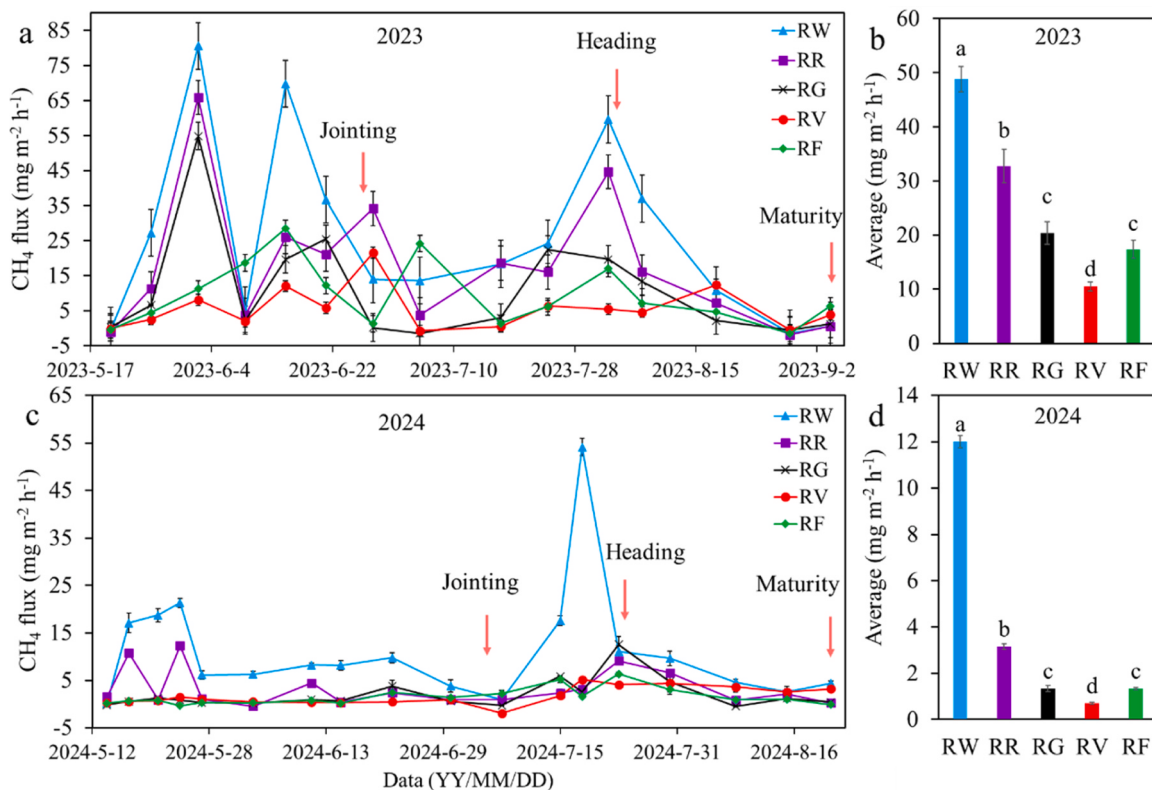


Fig. 4. CH_4 emission flux from rice fields under different crop rotation systems. RW: wheat-rice; RR: rapeseed-rice; RG: green vegetables-rice; RV: *Vicia villosa* var. rice.; RF: winter fallow field-rice. The error bars in the figure represent the standard deviation (STDEV). Different lowercase letters indicate significant differences between different crop rotation systems at the 0.05 level (LSD test).

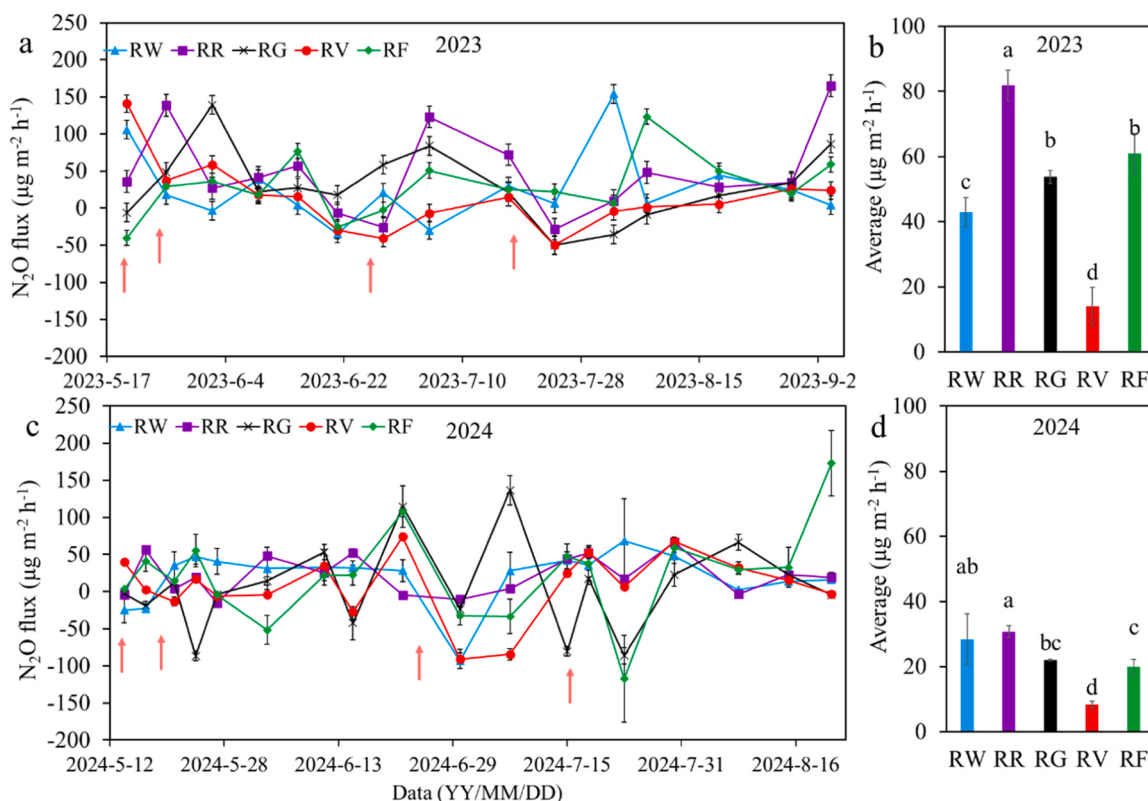


Fig. 5. N_2O emission flux from rice fields under different crop rotation systems. RW: wheat-rice; RR: rapeseed-rice; RG: green vegetables-rice; RV: *Vicia villosa* var. rice.; RF: winter fallow field-rice. The red arrow in the figure points to the fertilization date; The error bars in the figure represent the standard deviation (STDEV). Different lowercase letters indicate significant differences between different crop rotation systems at the 0.05 level (LSD test).

times higher than RF, and RV ($147.56 \text{ kg hm}^{-2}$) was the lowest. In 2024, RW and RR were 65.07 %–84.42 % lower than those in 2023 (Fig. 6a).

3.3. N_2O emissions

During the entire rice growing season, N_2O emission peaked around 7–15 days after nitrogen fertilizer application (Fig. 5). In 2023, the average N_2O emission flux of RR ($81.85 \mu\text{g m}^{-2} \text{ h}^{-1}$) was significantly higher than that of the other systems and was 4.82 times that of the RV ($14.06 \mu\text{g m}^{-2} \text{ h}^{-1}$) (Fig. 5b). In 2024, RR ($30.75 \mu\text{g m}^{-2} \text{ h}^{-1}$) and RW ($28.47 \mu\text{g m}^{-2} \text{ h}^{-1}$) did not show significant differences, being 54.52 % and 43.06 % higher than RF, respectively. In contrast, RV ($8.31 \mu\text{g m}^{-2} \text{ h}^{-1}$) was significantly lower by 58.24 % compared to RF (Fig. 5d). The total N_2O emission was significantly different from year to year. In 2024, there was a decrease in different crop rotation systems, and RF (68.95 %), RR (54.37 %), and RG (50.33 %) exhibited the most significant decrease (Fig. 6b).

3.4. Rice grain yield, GWP, and GHGI

During the 2024 growing season, rainfall decreased significantly, resulting in shorter durations of field flooding. Consequently, cumulative emissions of CH_4 and N_2O exhibited significant differences between the two years. However, the continuous incorporation of straw over two consecutive years enhanced the soil carbon pool in paddy fields and contributed to increased rice yields, leading to a significant difference in yield between the two years.

There are significant differences in yield between different years and different upland-paddy rotation systems. In 2023, RG (8660.91 kg hm^{-2}) exhibited the highest rice grain yield, which was 11.85 % greater than RF, the treatment with the lowest yield. The yields of the other treatments showed no significant differences. In 2024, the yield trend remained consistent with that of 2023; however, the yields in the second year increased by 6.31 %–13.37 % compared to the first year (Fig. 6c). Under different rotation systems, CH_4 was the main contributor to GWP. The

accounting for more than 92.87 % of GWP. In the two-year experiment, the GWP of RW ($11,687.43 \text{ kg CO}_2\text{-eq hm}^{-2}$) was significantly higher than that of the other treatments, being 2.13 times that of RF. The GWP of RR ($6882.14 \text{ kg CO}_2\text{-eq hm}^{-2}$) and RG ($4380.19 \text{ kg CO}_2\text{-eq hm}^{-2}$) was 84.84 % and 17.64 % higher than that of RF, respectively. The GWP of RV was 35.65 % lower than that of RF (Fig. 6d). The trend of GHGI change was consistent with that of GWP. RW ($1.48 \text{ kg CO}_2\text{-eq kg}^{-1}$ grain) was the highest, which was 2.02 times that of RF. RR ($0.91 \text{ kg CO}_2\text{-eq kg}^{-1}$ grain) and RG ($0.52 \text{ kg CO}_2\text{-eq kg}^{-1}$ grain) were 85.71 % and 6.12 % higher than RF, respectively. RV was 38.77 % lower than RF (Fig. 6e).

3.5. *mcrA*, *pmoA*, and *mcrA/pmoA*

Methanogens showed significant differences between the two years. In the two-year experiment, the abundance of methanogens in RW was significantly higher than that in other treatments during the whole rice growth period and increased by an average of 2.3 times from jointing to maturity, followed by RR, which increased by an average of 1.15 times. The abundance of methanogens in RG ($7.98 \times 10^6 \text{ copies g}^{-1}$ soil) and RV ($12.97 \times 10^6 \text{ copies g}^{-1}$ soil) peaked at the heading stage and stabilized at the maturity stage (Fig. 7a-c). The differences in methanotrophic bacterial communities during the jointing stage between the two years were significant, whereas no significant differences were observed between the heading and maturity stages. In 2023, RW exhibited a gradual increase with the progression of the rice growth period, reaching an increment of 1.26 times by the maturity stage. In 2024, RF showed the most substantial increase, reaching 3.8 times its initial value. The RR, RG, and RV systems peaked at the heading stage across both years of the experiment and subsequently declined gradually by the maturity stage (Fig. 7d-f). There was no significant difference in the changing trend of *mcrA/pmoA* during the jointing stage across years under different rotation systems, but significant differences were observed in both the heading and maturity stages. RW (1.73) was the highest during the jointing stage, 50.21 % higher than RF. The

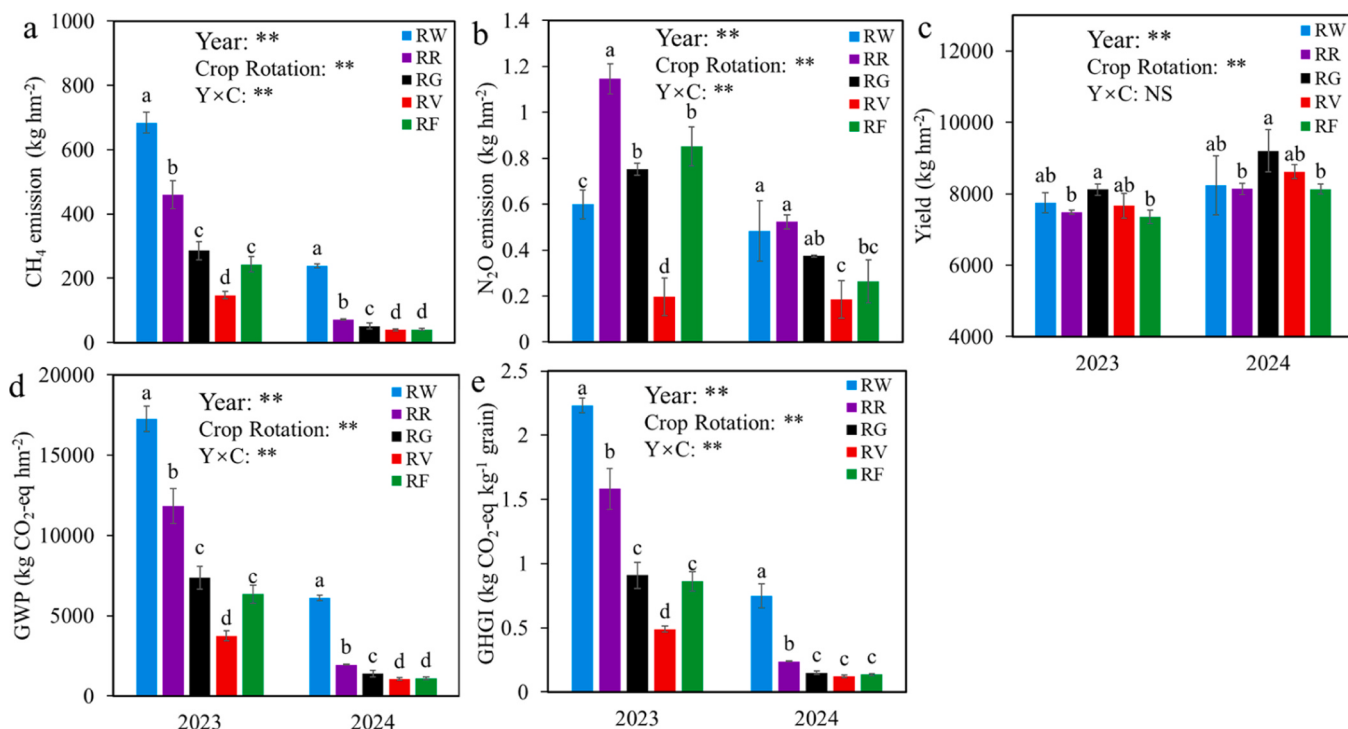


Fig. 6. The variations in cumulative emissions of CH_4 and N_2O , yields, GWP, and GHGI under different rotation systems. RW: wheat-rice; RR: rapeseed-rice; RG: green vegetables-rice; RV: *Vicia villosa* var.-rice.; RF: winter fallow field-rice. The error bars in the figure represent the standard deviation (STDEV). Different lowercase letters indicate significant differences between different crop rotation systems at the 0.05 level (LSD test).

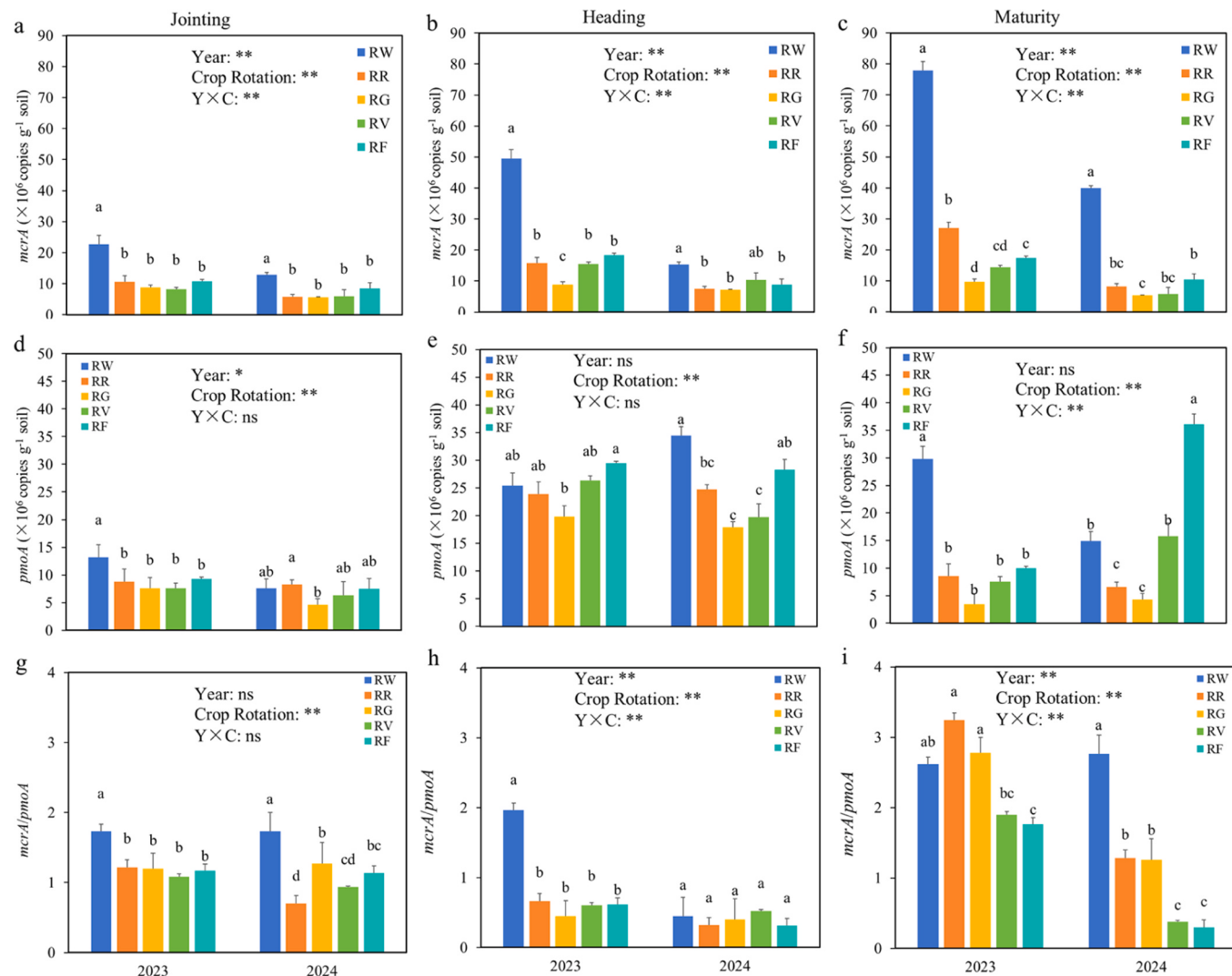


Fig. 7. Abundance of CH₄-related genes at different growth stages of rice season under different rotation systems. RW: wheat-rice; RR: rapeseed-rice; RG: green vegetables-rice; RV: *Vicia villosa* var.-rice.; RF: winter fallow field-rice. The error bars in the figure represent the standard deviation (STDEV). Different lowercase letters indicate significant differences between different crop rotation systems at the 0.05 level (LSD test).

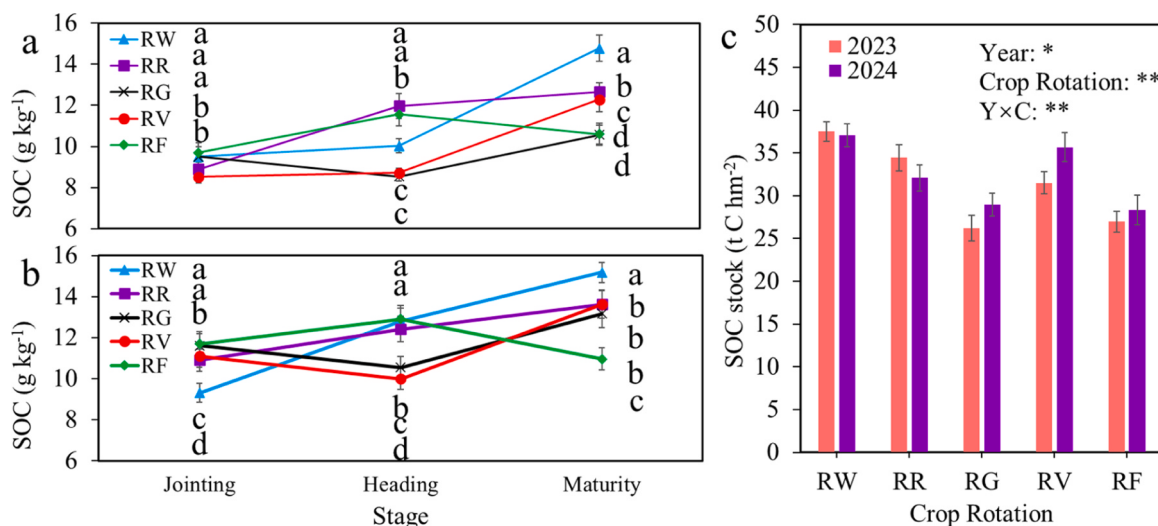


Fig. 8. SOC changes in rice fields under different crop rotation systems. RW: wheat-rice; RR: rapeseed-rice; RG: green vegetables-rice; RV: *Vicia villosa* var.-rice.; RF: winter fallow field-rice. The error bars in the figure represent the standard deviation (STDEV). Different lowercase letters indicate significant differences between different crop rotation systems at the 0.05 level (LSD test).

difference between RV (0.93) and RF (1.15) in the mature stage was not significant and was significantly lower than RW (3.03), RR (2.70), and RG (1.98) (Fig. 7g-i).

3.6. Soil chemical properties

The soil organic carbon content exhibited an overall increasing trend throughout the rice growth period. In 2023, during the jointing stage, RW (9.49 g kg^{-1}), RG (9.49 g kg^{-1}), and RF (9.70 g kg^{-1}) were significantly higher than RR (8.89 g kg^{-1}), and RV (8.51 g kg^{-1}). This discrepancy likely reflects the early-stage organic matter accumulation advantages of RW, RG, and RF, which may be associated with root activity and microbial processes that enhance soil carbon retention. From the jointing stage to maturity, SOC in RW, RR, and RV systems increased by 55.57 %, 42.29 %, and 44.22 %, respectively, surpassing the growth rates of RG (11.22 %) and RF (9.16 %) (Fig. 8a). After two consecutive years of crop rotation, the soil carbon pool decreased by 1.19 % and 6.83 % under high C/N straw-return systems (RW and RR), attributed to carbon loss from elevated CH_4 emissions. In contrast, the low C/N RV system increased the carbon pool by 13.15 % due to reduced mineralization, while RG exhibited no significant difference compared to RF owing to limited straw input. Additionally, the highest soil NO_3^- -N content under RW ($18.67\text{--}20.95 \text{ mg kg}^{-1}$) strongly promoted N_2O emissions, whereas RV exhibited the lowest NO_3^- -N levels ($11.49\text{--}11.80 \text{ mg kg}^{-1}$), demonstrating significant mitigation potential (Fig. 9a-c, Fig. 6b).

4. Discussion

4.1. Effects of different crop rotation systems on CH_4 emissions in rice season

Different upland-paddy rotation systems significantly influenced CH_4 emissions during the rice-growing season, primarily mediated by variations in the C/N ratio of returned straw. Although prior studies have investigated CH_4 emissions under various rice rotation systems (Jiang et al., 2022; Van Dung et al., 2023; Xu et al., 2028), investigations specifically addressing upland-paddy rotations, particularly the effects of dry-season crop residue incorporation into paddy fields, remain scarce. In this study, significant differences in both CH_4 and N_2O emissions were observed among rotation systems. The wheat-rice (RW) and rapeseed-rice (RR) rotations exhibited higher straw C/N ratios (Fig. 3d), leading to rapid decomposition of residues during the early stages of rice growth. This process provided abundant carbon substrates for methanogens, thereby enhancing CH_4 emissions. The RW system produced the highest CH_4 emissions, whereas the RR system exhibited both high CH_4

and the highest N_2O emissions (Fig. 4b, d; Fig. 5b, d). This phenomenon can be attributed to two key factors: (1) the high C/N ratio of returned straw (0.53**) (Fig. 10), and (2) significantly higher soil nitrate content under RR (Fig. 9c), which, as a substrate for denitrification (Dyer and Desjardins, 2006), promoted N_2O accumulation (Fig. 5). Although studies by Ma and Shen have suggested that straw returning generally reduces N_2O emissions through the immobilization of mineral nitrogen and the reduction of nitrification-denitrification substrates (Shen et al., 2014; Ma et al., 2019), the elevated nitrate levels observed in RR may be related to high fertilizer input and rapid N turnover. Furthermore, under flooded conditions, the oxygen consumption during decomposition of returned wheat straw is 1–3 times higher than in no-straw treatments (Wei et al., 2019; Guo et al., 2021), rapidly lowering redox potential (Eh), with the extent of reduction positively correlated with the straw input rate (Fig. 10). This low-Eh environment not only enhances *mcrA* gene abundance but also facilitates the reduction of N_2O to N_2 , resulting in a “high CH_4 -low N_2O ” emission pattern in the RW system (Ma et al., 2019; Lin et al., 2023).

From a microbial perspective, CH_4 emissions are primarily governed by the activity and abundance of methanogens and methanotrophs. Methanogens are the dominant biological source of CH_4 in paddy soils, while methanotrophs metabolize CH_4 as their sole carbon and energy source (Kim et al., 2013). As rice grows, the progressive decomposition of returned straw—especially high-C/N wheat and rapeseed residues—enhances carbon availability for methanogens. Consequently, RW and RR systems exhibited higher seasonal mean abundances of the *mcrA* gene and *mcrA/pmoA* ratios (Fig. 7g-i), indicating that high-C/N straw stimulates methanogens more than methanotrophs, thereby exacerbating CH_4 production.

In contrast, the RV, RG, and RF systems exhibited significantly lower CH_4 emissions. In the RV system, straw C/N was only 11.28, and Vicia was incorporated two months before rice transplanting. This allowed for partial decomposition before flooding, reducing oxygen depletion during early anaerobic conditions and maintaining a more oxidized soil environment. As a result, *mcrA* abundance decreased, *pmoA* abundance increased, and the *mcrA/pmoA* ratio was the lowest among treatments (Fig. 7), supporting its CH_4 -suppressing potential and confirming our second hypothesis. In the RF system (winter fallow), CH_4 emissions remained the lowest due to minimal carbon input, while the RG treatment did not significantly differ from RF due to limited biomass return from vegetable residues. Additionally, interannual climatic variation strongly affected GHG emissions. Compared to 2023, reduced precipitation in 2024 resulted in a shorter flooding period and constrained Eh reduction (Zhou et al., 2024a), significantly decreasing CH_4 emissions (by 65.07–84.42 %), especially in RW and RR treatments, which initially exhibited the highest emission fluxes. Regional variation followed

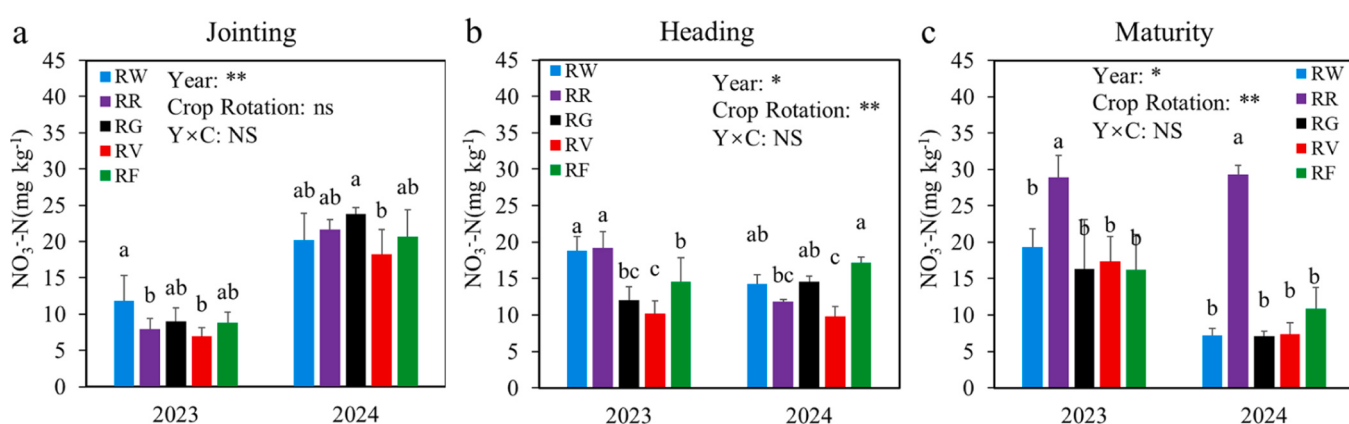


Fig. 9. Nitrate nitrogen content in the soil during the rice season under different crop rotation systems. RW: wheat-rice; RR: rapeseed-rice; RG: green vegetables-rice; RV: *Vicia villosa* var.-rice.; RF: winter fallow field-rice. The error bars in the figure represent the standard deviation (STDEV). Different lowercase letters indicate significant differences between different crop rotation systems at the 0.05 level (LSD test).

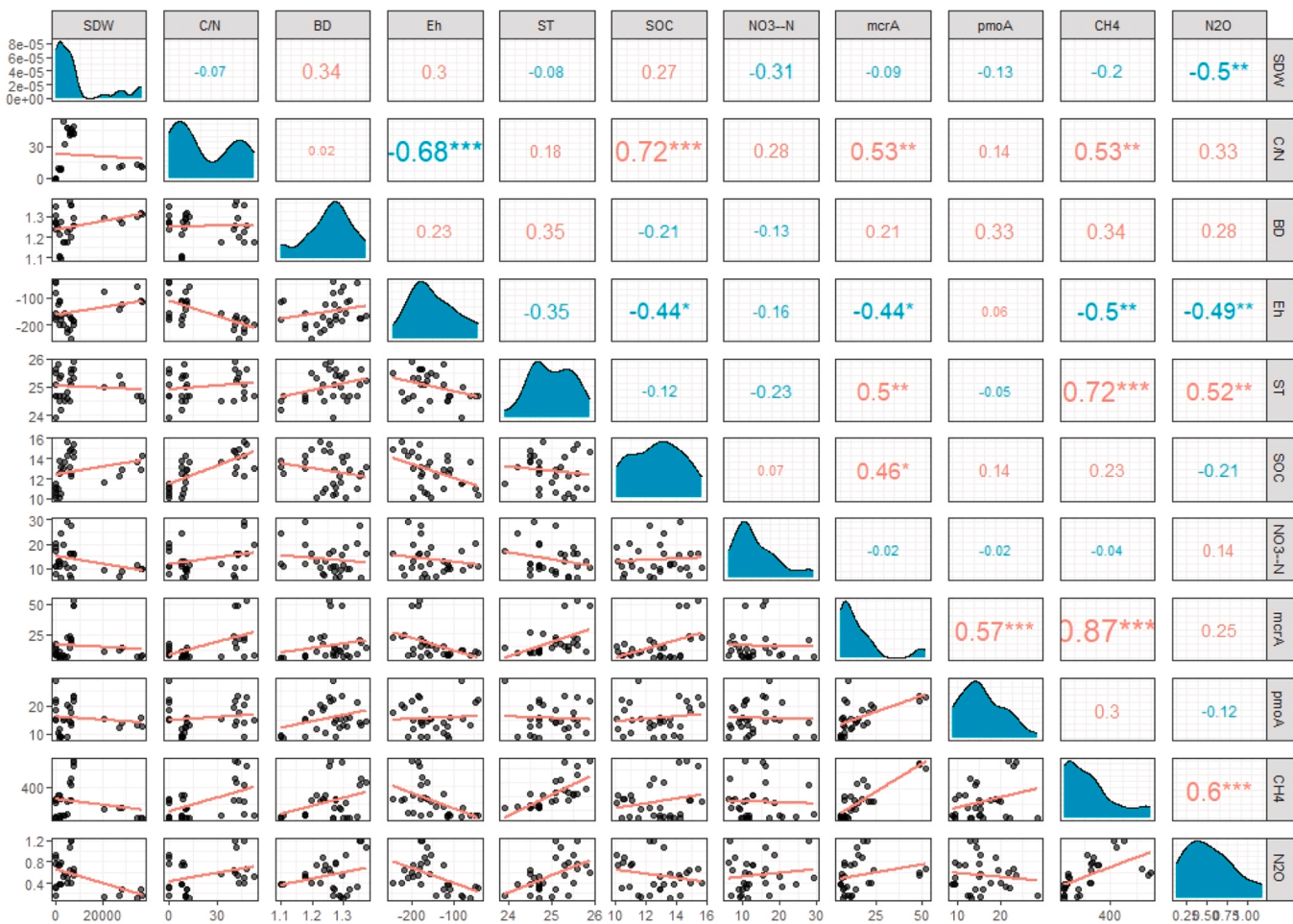


Fig. 10. Pearson correlation analysis showing the relationships between soil properties, straw return parameters, gene abundances, and CH₄ and N₂O emissions. SOC: soil organic carbon; BD: bulk density; Eh: electrode potential; ST: soil temperature; SDW: dry weight of returned straw; SCC: straw carbon accumulation; SNC: straw nitrogen accumulation; C/N: SCC/SNC. ***, **, and *** indicated $p < 0.05$, $p < 0.01$, and $p < 0.001$, respectively.

similar patterns: in South China, hot and humid conditions accelerate the decomposition of low-C/N straw and further reduce the *mcrA*/*pmoA* ratio, whereas arid and semi-arid regions experience limited methanogen activity due to water scarcity (Zhou et al., 2020), leading to lower mitigation potential compared to the findings reported in our study.

Further analysis revealed a strong positive correlation between straw C/N ratio and soil organic carbon (SOC) ($r = 0.77***$). At the same time, SOC was positively associated with *mcrA* gene abundance ($r = 0.46^*$) and CH₄ emissions ($r = 0.52^{**}$) (Fig. 10). These findings suggest that carbon input during straw decomposition is a key driver of CH₄ generation, whereas low nitrogen levels contribute to the suppression of N₂O emissions. High-C/N systems (RW, RR) enhanced SOC but also significantly increased CH₄ emissions. In contrast, the low-C/N RV system achieved a synergistic outcome, balancing carbon accumulation and GHG reduction, resulting in a net reduction of CH₄ and N₂O fluxes. This C–N coordination mechanism provides important theoretical support for optimizing rice rotation and straw return strategies in climate-smart agriculture.

4.2. Effects of crop rotation systems on rice grain yield and GHGI

The primary differences among the crop rotation systems lie in the selection of upland crops and the corresponding agronomic practices during the dry season, while rice cultivation practices during the wet season remain consistent. These differences significantly influence both rice yield and methane emissions by altering soil carbon and nitrogen inputs, as well as straw-return strategies (Wang et al., 2024). In the

upland-paddy rotation systems commonly used in southern China, complete straw return of winter crops is widely adopted (Liu et al., 2019). As a carbon-rich organic material, straw decomposition not only provides nutrients for crops (Wang et al., 2023) but also significantly increases the soil organic carbon stock through microbial transformation and mineral protection mechanisms (Zhang et al., 2024), thereby improving nutrient retention and supporting better crop growth conditions (Islam et al., 2022). However, different straw-return practices (e.g., no-tillage, plowing, trench burial) and regional climatic conditions significantly affect the rate of straw decomposition and the intensity of greenhouse gas emissions (Guo et al., 2021). For example, plowing, which is widely adopted in practice, thoroughly incorporates straw into the soil, creating anaerobic conditions that enhance CH₄ emissions. In contrast, no-tillage practices tend to result in lower CH₄ emissions. The effects of trench burial remain debated due to potential water accumulation in trenches that fosters reductive conditions. In cold regions, such as Xinjiang and Northeast China, low temperatures limit decomposition, making the increase in CH₄ less pronounced despite higher straw input. However, in warm and humid southern areas, such as Sichuan, straw return significantly increases CH₄ emissions (Li et al., 2024).

Compared with winter fallow, planting astragalus or potatoes during the dry season significantly increased SOC content in paddy fields (Zhou et al., 2024b). In the astragalus-rice system, the low C/N ratio and high organic matter content of astragalus contributed to greater carbon input without substantially increasing CH₄ emissions, achieving a balance between mitigation and carbon sequestration. In contrast, the potato-rice system had high nitrogen fertilizer inputs, which increased

SOC but also led to higher N₂O emissions. Some studies suggest that the potato–rice rotation may accumulate less SOC than winter fallow (Aumtong et al., 2023), possibly due to differences in crop type, straw C/N ratio (Zhou et al., 2024b), and straw-induced microbial activation accelerating SOC mineralization (Liang et al., 2018). A meta-analysis showed that soil carbon accumulation becomes more significant when the soil C/N ratio surpasses 20 (Xin et al., 2024), consistent with the higher SOC observed in the RW and RR systems (Fig. 8a, b). However, whether increased SOC offsets the warming potential from CH₄ depends on the equilibrium between greenhouse gas emission intensity and crop productivity.

Long-term field trials further confirmed that the greenhouse gas mitigation effect of rotation systems is cumulative. In the Yangtze River Basin, continuous RV rotation significantly enhanced annual SOC sequestration rates, outperforming RW in the long term. Moreover, its GHGI decreased annually, indicating the long-term carbon sequestration and emission reduction potential of low-C/N systems in subtropical paddy regions (Chen et al., 2016; Yue et al., 2023). In our two-year trial, SOC content increased by 13.15 % across all treatments (Fig. 8), accompanied by a simultaneous increase in rice yield, suggesting that the advantages of rotation systems can be sustained over time. Inter-annual climatic variation exerted a substantial regulatory effect on emission fluxes. In 2024, reduced rainfall shortened waterlogging periods and weakened the decline in soil redox potential, thereby suppressing CH₄ formation and leading to reduced CH₄ and N₂O emissions compared to 2023. The significant increase in rice yield after two years of rotation may be attributed to the gradual release of nutrients from returned straw and the increase in SOC. Among different systems, RG achieved the highest yield, followed by RV, while RW and RR exhibited slightly lower yields. The elevated yield in RG may be attributed to the elevated soil residual nitrogen resulting from greater fertilizer input in the dry season, though this also increased N₂O emissions. Conversely, RV maintained stable yields despite lower nitrogen input due to high levels of straw-derived carbon and nitrogen that contributed to increased soil organic matter. CH₄ was the dominant contributor to the GWP in this study. The RW and RR systems, characterized by their substantial CH₄ emissions and lower yields, exhibited the highest GHGI. In contrast, the RG and RV rotations achieved a desirable balance of low CH₄ emissions and high yields, resulting in lower GHGI and more favorable carbon efficiency, thus providing support for our third hypothesis.

Under current pressures such as high population density, dependence on oilseed imports, and strict farmland protection policies, the RW and RR systems are likely to remain significant in agricultural production throughout southern China. Therefore, optimizing fertilization regimes, improving water management, or innovating straw-return techniques to reduce GHGI in these systems will be a crucial direction for future research and technology development. At the same time, despite the advantages of RG and RV in yield and emissions, their sustainability challenges—such as excessive fertilizer use during the vegetable season (RG) or reduced economic returns from single-season rice cultivation (RV)—hinder their capacity to fully align with China's long-term food security and farmland protection objectives.

5. Conclusion

This study elucidated the synergistic regulatory mechanism of straw C/N ratio on methane emissions, crop yield, and carbon efficiency in rice-based rotation systems. Straw with a low C/N ratio (e.g., RV) effectively reduced CH₄ emissions and maintained stable yields by optimizing the *mcrA/pmoA* ratio, thereby significantly lowering the GHGI. In contrast, high C/N systems (RW and RR) promoted soil carbon accumulation but substantially increased CH₄ emissions, leading to relatively elevated GHGI. Although the RV and RG rotations demonstrated substantial potential for emission reduction and efficiency enhancement, challenges such as excessive fertilizer application during

the non-rice season or limited productivity remain. Considering the predominant role of RW and RR systems in contemporary agricultural practices, future efforts should prioritize the integrated optimization of precision fertilization and straw management technologies and explore *Vicia villosa* var.–crop intercropping systems during the non-rice season in RV to jointly achieve the sustainable development goals of emission reduction, efficiency improvement, and yield enhancement.

Funding

This work was supported by the National Key Research and Development Program (2023YFD2301901, 2024YFD2300401), the Natural Science Foundation of Sichuan Province (2024NZZJ0003, 2023YFN0046), The Chengdu Agricultural Science and Technology Center Program (NASC2024KY10)

CRediT authorship contribution statement

Yuanqing Shi: Resources. **Jun Ma:** Supervision, Writing – review & editing, Funding acquisition, Project administration. **Leilei Li:** Validation. **Zhiyuan Yang:** Supervision, Conceptualization, Funding acquisition, Project administration. **Qingyue Cheng:** Investigation, Validation. **Qin Liao:** Software, Investigation. **Zhonglin Wang:** Visualization. **Hongkun Xie:** Investigation, Data curation. **Yongjian Sun:** Methodology. **Yu Li:** Visualization. **Zongkui Chen:** Conceptualization, Supervision. **Binbin Liu:** Investigation. **Na Li:** Methodology, Formal analysis, Funding acquisition. **Chuanhai Shu:** Investigation, Data curation, Writing – original draft. **Feijie Li:** Investigation, Visualization. **Qiqi Chen:** Investigation, Resources.

Declaration of Competing Interest

The authors declare that they have no known competing financial interests or personal relationships that could have appeared to influence the work reported in this paper.

Acknowledgments

We appreciate essentialslink (www.esentialslink.cn) for English language editing.

Data availability

Data will be made available on request.

References

- Aumtong, S., Chotamonsak, C., Glomchinda, T., 2023. Study of the interaction of dissolved organic carbon, available nutrients, and clay content driving soil carbon storage in the rice rotation cropping system in Northern Thailand. *Agro. J.* 13, 142. <https://doi.org/10.3390/agronomy13010142>.
- Cha-un, N., Chidthaisong, A., Yagi, K., Sudo, S., Towprayoon, S., 2017. Greenhouse gas emissions, soil carbon sequestration and crop yields in a rain-fed rice field with crop rotation management. *Agr. Ecosyst. Environ.* 237, 109–120. <https://doi.org/10.1016/j.agee.2016.12.025>.
- Chen, S., Xu, C., Yan, J., Zhang, X., Zhang, X., Wang, D., 2016. The influence of the type of crop residue on soil organic carbon fractions: an 11-year field study of rice-based cropping systems in southeast China. *Agr. Ecosyst. Environ.* 223, 261–269. <https://doi.org/10.1016/j.agee.2016.03.009>.
- Chivenge, P., Vanlauwe, B., Gentile, R., Six, J., 2011. Organic resource quality influences short-term aggregate dynamics and soil organic carbon and nitrogen accumulation. *Soil Biol. Biochem.* 43, 657–666. <https://doi.org/10.1016/j.soilbio.2010.12.002>.
- Deng, Z., Ren, X., Han, J., Cui, K., Han, K., Yue, Q., Zhou, J., Zhai, Z., Xiong, D., Yuan, S., Huang, J., Peng, S., 2024. Identifying a sustainable rice-based cropping system via on-farm evaluation of grain yield, carbon sequestration capacity and carbon footprints in Central China. *Field Crop. Res.* 316, 109510. <https://doi.org/10.1016/j.fcr.2024.109510>.
- Ding, Y.-G., Chen, L., Dong, J.-X., Zhu, M., Li, C.-Y., Zhu, X.-K., Ding, J.-F., Guo, W.-S., 2022. Characteristics of yield components, nitrogen accumulation and translocation, and grain quality of semi-winter cultivars with high-yield and high-efficiency. *Acta Agro. Sin.* 48, 11. <https://doi.org/10.3724/SP.J.1006.2022.11117>.

- Dong, Q., Dong, Y., Li, W., Xie, C., Li, C., Zhang, M., Chen, C., Zhang, A., 2023. Effects of different green manures on soil fertility and nutrient uptake of rice. *Soils* 55, 554–561. <https://doi.org/10.13758/j.cnki.tr.2023.03.012>.
- Dyer, J.A., Desjardins, R.L., 2006. Carbon dioxide emissions associated with the manufacturing of tractors and farm machinery in Canada. *Biosyst. Eng.* 93, 107–118. <https://doi.org/10.1016/j.biosystemseng.2005.09.011>.
- Fang, Y.-T., Ren, T., Zhang, S.-T., Zhou, X.-Q., Zhao, J., Liao, S.-P., Cong, R.-H., Lu, J.-W., 2023. Different effects of nitrogen, phosphorus and potassium fertilizers on oilseed rape yield and nutrient utilization between continuous upland and paddy-upland rotations. *Acta Agro. Sin.* 49, 772–783. <https://doi.org/10.3724/SP.J.1006.2023.24061>.
- Guo, L., Zhang, L., Liu, L., Sheng, F., Cao, C., Li, C., 2021. Effects of long-term no tillage and straw return on greenhouse gas emissions and crop yields from a rice-wheat system in central China. *Agr. Ecosyst. Environ.* 322, 107650. <https://doi.org/10.1016/j.agee.2021.107650>.
- Hou, H., Yang, S., Wang, F., Li, D., Xu, J., 2016. Controlled irrigation mitigates the annual integrative global warming potential of methane and nitrous oxide from the rice–winter wheat rotation systems in Southeast China. *Eco Eng.* 86, 239–246. <https://doi.org/10.1016/j.ecoleng.2015.11.022>.
- IPCC, 2014. Climate Change 2014 – the physical science basis: working group I Contribution to the Fifth Assessment Report of the Intergovernmental Panel on Climate Change. Series. Cambridge. <https://doi.org/10.1017/CBO9781107415324>.
- IPCC, 2014. Climate Change 2014: synthesis report. Contribution of Working Groups I, II and III to the Fifth Assessment Report of the Intergovernmental Panel on Climate Change [Core Writing Team, R.K. Pachauri and L.A. Meyer (eds.)]. Series. Geneva, Switzerland. <https://www.ipcc.ch/report/ar5/syr/>.
- IPCC, 2023. Climate Change 2021 – The Physical Science Basis: Working Group I Contribution to the Sixth Assessment Report of the Intergovernmental Panel on Climate Change. Cambridge University Press, Cambridge.
- Islam, M.U., Guo, Z., Jiang, F., Peng, X., 2022. Does straw return increase crop yield in the wheat-maize cropping system in China? A meta-analysis. *Field Crop. Res.* 279, 108447. <https://doi.org/10.1016/j.fcr.2022.108447>.
- Jiang, M., Xu, P., Wu, L., Zhao, J., Wu, H., Lin, S., Yang, T., Tu, J., Hu, R., 2022. Methane emission, methanogenic and methanotrophic communities during rice-growing seasons differ in diversified rice rotation systems. *Sci. Total Environ.* 842, 156781. <https://doi.org/10.1016/j.scitotenv.2022.156781>.
- Kan, Z.-R., Li, Y., Yang, X., Zhai, S., Meng, Y., Xu, C., Qi, J., Li, F.-M., Chen, C., Yang, H., 2023. Methane emission under straw return is mitigated by tillage types depending on crop growth stages in a wheat-rotated rice farming system. *Soil Till. Res.* 228, 105649. <https://doi.org/10.1016/j.still.2023.105649>.
- Kim, S.Y., Lee, C.H., Gutierrez, J., Kim, P.J., 2013. Contribution of winter cover crop amendments on global warming potential in rice paddy soil during cultivation. *Plant Soil* 366, 273–286. <https://doi.org/10.1007/s11104-012-1403-4>.
- Li, R.-C., Tian, Y.-G., Wang, F., Sun, Y.-F., Lin, B.-J., Dang, Y.-P., Zhao, X., Zhang, H.-L., Xu, Z.-Y., 2024. Optimizing the rate of straw returning to balance trade-offs between carbon emission budget and rice yield in China. *Sustain Prod. Consum.* 47, 166–177. <https://doi.org/10.1016/j.spc.2024.03.026>.
- Liang, J., Zhou, Z., Huo, C., Shi, Z., Cole, J.R., Huang, L., Konstantinidis, K.T., Li, X., Liu, B., Luo, Z., Penton, C.R., Schuur, E.A.G., Tiedje, J.M., Wang, Y.-P., Wu, L., Xia, J., Zhou, J., Luo, Y., 2018. More replenishment than priming loss of soil organic carbon with additional carbon input. *Nat. Commun.* 9, 3175. <https://doi.org/10.1038/s41467-018-05667-7>.
- Lin, J., Xu, Z., Xue, Y., Sun, R., Yang, R., Cao, X., Li, H., Shao, Q., Lou, Y., Wang, H., Yang, Q., Pan, H., Zhuge, Y., 2023. N2O emissions from soils under short-term straw return in a wheat-corn rotation system are associated with changes in the abundance of functional microbes. *Agr. Ecosyst. Environ.* 341, 108217. <https://doi.org/10.1016/j.agee.2022.108217>.
- Lin, S., Yin, M., Chu, G., Xu, C., Wang, D., Zhang, X., Chen, S., 2019. Effects of various paddy-upland crop rotations and nitrogen fertilizer levels on CH4 emission in the middle and lower reaches of the Yangtze river. *Sci. Agric. Sin.* 52, 2484–2499. <https://doi.org/10.3864/j.issn.0578-1752.2019.14.008>.
- Luton, P.E., Wayne, J.M., Sharp, R.J., Riley, P.W., 2002. The mcrA gene as an alternative to 16S rRNA in the phylogenetic analysis of methanogen populations in landfill. *Microbiology* 148, 3521–3530. <https://doi.org/10.1099/00221287-148-11-3521>.
- Ma, Y., Liu, D.L., Schwenke, G., Yang, B., 2019. The global warming potential of straw-return can be reduced by application of straw-decomposing microbial inoculants and biochar in rice-wheat production systems. *Environ. Pollut.* 252, 835–845. <https://doi.org/10.1016/j.envpol.2019.06.006>.
- Paul, E.A., 2015. *Soil Microbiology, Ecology and Biochemistry*. Academic Press, Burlington.
- Peng, Y., Liu, Y., Miao, Y., 2021. A numerical study on impacts of greenhouse gases on Asian summer monsoon. *J. Appl. Meteorol. Sci.* 32, 245–256. <https://doi.org/10.11988/1001-7313.20210209>.
- Raheema, A., Zhang, J., Jing Huangb, C., Yu Jiangc, D., Siddika, M.A., Dengd, A., Jusheng Gaob, C., Zhang, W., 2019. Greenhouse gas emissions from a rice-rice-green manure cropping system in South China. *Geoderma* 331–339. <https://doi.org/10.1016/j.geoderma.2019.07.007>.
- Salahin, N., Alam, M.K., Islam, M.M., Naher, L., 2013. Effects of green manure crops and tillage practice on maize and rice yields and soil properties. *Aust. J. Crop Sci.* 7 <https://search.informit.org/doi/10.3316/informit.669075287954321>.
- Shen, J., Tang, H., Liu, J., Wang, C., Li, Y., Ge, T., Jones, D.L., Wu, J., 2014. Contrasting effects of straw and straw-derived biochar amendments on greenhouse gas emissions within double rice cropping systems. *Agr. Ecosyst. Environ.* 188, 264–274. <https://doi.org/10.1016/j.agee.2014.03.002>.
- Song, Y., Li, J., Gu, H.-H., Lu, Z.-F., Liao, S.-P., Li, X.-K., Cong, R.-H., Ren, T., Lu, J.-W., 2023. Effects of application of nitrogen on seed yield and quality of winter oilseed rape(*Brassica napus L.*). *Acta Agro. Sin.* 49, 2002–2011. <https://doi.org/10.3724/SP.J.1006.2023.24179>.
- Tang, H., Xiao, X., Tang, W., Wang, K., Sun, J., Li, W., Yang, G., 2015. Effects of winter covering crop residue incorporation on CH4 and N2O emission from double-cropped paddy fields in southern China. *Environ. Sci. Pollut. R.* 22, 12689–12698. <https://doi.org/10.1007/s11356-015-4557-9>.
- Tuomivirta, T.T., Yrjälä, K., Fritze, H., 2009. Quantitative PCR of pmoA using a novel reverse primer correlates with potential methane oxidation in Finnish fen. *Res. Microbiol.* 160, 751–756. <https://doi.org/10.1016/j.resmic.2009.09.008>.
- Van Dung, T., Thu Nguyen, K., Ho, P.N.H., Lich Duong, T.N., Vu, T.N.M., Nguyen, L.T.P., Van, V.L., MacDonald, B., 2023. Reducing greenhouse gas emission by alternation of the upland crop rotation in the Mekong Delta, Vietnam. *Soil. Water Res.* 18, 16–24.
- Wang, T., Ji, C., Zhou, W., Chen, H., Chen, Y., Liu, Q., Cao, T., Jin, C., Song, W., Deng, F., Lei, X., Tao, Y., Fu, S., Ren, W., 2024. Greenhouse gas emissions during the rice season are reduced by a low soil C:N ratio using different upland-paddy rotation systems. *Field Crop. Res.* 317, 109562. <https://doi.org/10.1016/j.fcr.2024.109562>.
- Wang, H., Shen, M., Hui, D., Chen, J., Sun, G., Wang, X., Lu, C., Sheng, J., Chen, L., Luo, Y., Zheng, J., Zhang, Y., 2019. Straw incorporation influences soil organic carbon sequestration, greenhouse gas emission, and crop yields in a Chinese rice (*Oryza sativa L.*)–wheat (*Triticum aestivum L.*) cropping system. *Soil Till. Res.* 195, 104377. <https://doi.org/10.1016/j.still.2019.104377>.
- Wang, Z., Tang, H., Huang, G., Miao, J., Liu, Y., Shah, A.N., Nawaz, M., Ayub, M.A., Hassan, M.U., 2023. Different rotation and double straw returning significantly increase liable organic carbon content and yield of double cropping paddy field in Southern China. *Int. J. Plant Prod.* 17, 681–691. <https://doi.org/10.1007/s42106-023-00265-0>.
- Wang, H., Zhang, D., Zhang, Y., Zhai, L., Yin, B., Zhou, F., Geng, Y., Pan, J., Luo, J., Gu, B., 2018. Ammonia emissions from paddy fields are underestimated in China. *Environ. Pollut.* 235, 482–488. <https://doi.org/10.1016/j.envpol.2017.12.103>.
- Wei, Q., Xu, J., Sun, L., Wang, H., Lv, Y., Li, Y., Hameed, F., 2019. Effects of straw returning on rice growth and yield under water-saving irrigation. *Chil. J. Agric. Res.* 79, 66–74. <https://doi.org/10.4067/S0718-58392019000100066>.
- WMO, 2020. Greenhouse gas bulletin: the state of greenhouse gases in the atmosphere based on global observations through 2020. Series. <https://wmo.int/publications-series/greenhouse-gas-bulletin>.
- Wu, Y.-H., Hao, X.-S., Tian, X.-H., Chen, H., Zhang, C.-H., Cui, Y.-Z., Qin, Y.-H., 2020b. Effect of straw returning combined with NPK fertilization on soil carbon sequestration and economic benefits under rice-wheat rotation in Hanzhong basin. *Acta Agro. Sin.* 46, 259–268. <https://doi.org/10.3724/SP.J.1006.2020.92013>.
- Wu, X., Jiang, Z., Lu, Z., Lu, G., Xu, Y., Shi, W., Min, J., 2020a. Effects of the partial replacement of chemical fertilizer with manure on the yield and nitrogen emissions in leafy vegetable production. *Chin. J. Eco-Agric.* 28, 349–356. <https://doi.org/10.13930/j.cnki.cjea.190761>.
- Wu, Z., Lai, X., Li, K., 2021. Water quality assessment of rivers in Lake Chaohu Basin (China) using water quality index. *Ecol. Indic.* 121, 107021. <https://doi.org/10.1016/j.ecolind.2020.107021>.
- Xie, W., He, P., Ma, H.-L., Lei, F., Huang, X.-L., Fan, G.-Q., YANG, H.-K., 2023. Effects of straw mulching from autumn fallow and phosphorus application on nitrogen uptake and utilization of winter wheat. *Acta Agro. Sin.* 50, 440–450. <https://doi.org/10.3724/SP.J.1006.2024.31019>.
- Xin, J., Yan, L., Cai, H., 2024. Response of soil organic carbon to straw return in farmland soil in China: a meta-analysis. *J. Environ. Manag.* 359, 121051. <https://doi.org/10.1016/j.jenvman.2024.121051>.
- Xu, P., Jiang, M., Khan, I., Muhammad, S., Zhao, J., Yang, T., Hu, R., 2023. The effect of upland crop planting on field N2O emission from rice-growing seasons: a case study comparing rice-wheat and rice-rape seed rotations. *Agr. Ecosyst. Environ.* 347, 108365. <https://doi.org/10.1016/j.agee.2023.108365>.
- Xu, P., Mengdie, J., Khan, I., Shaaban, M., Zhao, J., Yang, T., Hu, R., 2028. The effect of upland crop planting on field N2O emission from rice-growing seasons: A case study comparing rice-wheat and rice-rape seed rotations. *Agr. Ecosyst. Environ.* 347, 108365. <https://doi.org/10.1016/j.agee.2023.108365>.
- Yang, Y.-L., Shen, L.-d., Zhao, X., Shan, J., Wang, S.-w., Zhou, W., Liu, J.-q., Liu, X., Tian, M.-h., Yang, W.-t., Jin, J.-h., Wu, H.-s., 2022. Long-term incorporation of wheat straw changes the methane oxidation potential, abundance and community composition of methanotrophs in a paddy ecosystem. *Appl. Soil Ecol.* 173, 104384. <https://doi.org/10.1016/j.apsoil.2021.104384>.
- Yanni, S.F., Whalen, J.K., Simpson, M.J., Janzen, H.H., 2011. Plant lignin and nitrogen contents control carbon dioxide production and nitrogen mineralization in soils incubated with Bt and non-Bt corn residues. *Soil Biol. Biochem.* 43, 63–69. <https://doi.org/10.1016/j.soilbio.2010.09.012>.
- Yue, Q., Sun, J., Hillier, J., Sheng, J., Guo, Z., Zhu, P., Cheng, K., Pan, G., Li, Y., Wang, X., 2023. Green manure rotation and application increase rice yield and soil carbon in the Yangtze River valley of China. *Pedosphere* 33, 589–599. <https://doi.org/10.1016/j.pedsph.2022.11.009>.
- Yuesi, W., Yinghong, W., 2003. Quick measurement of CH4, CO2 and N2O emissions from a short-plant ecosystem. *Adv. Atmos. Sci.* 20, 842–844. <https://doi.org/10.1007/BF02915410>.
- Zhang, X., Bi, J., Sun, H., Zhang, J., Zhou, S., 2019. Greenhouse gas mitigation potential under different rice-crop rotation systems: from site experiment to model evaluation. *Clean. Technol. Environ.* 21, 1587–1601.
- Zhang, S., Ren, T., Cong, W.-F., Fang, Y., Zhu, J., Zhao, J., Cong, R., Li, X., Lu, J., 2024. Oilseed rape-rice rotation with recommended fertilization and straw returning enhances soil organic carbon sequestration through influencing macroaggregates and molecular complexity. *Agr. Ecosyst. Environ.* 367, 108960. <https://doi.org/10.1016/j.agee.2024.108960>.

- Zhang, Y., Zhou, W., Chen, L., Wang, Z., Zhu, P., Sheng, J., Zheng, J., 2013. Methane and nitrous oxide emission under different paddy-upland crop rotation systems during rice growth season in Taihu Lake Region. *Chin. J. Eco-Agric.* 290–296. <https://doi.org/10.3724/SP.J.1011.2013.00290>.
- Zheng, H., Huang, H., Zhang, C., Li, J., 2016. National-scale paddy-upland rotation in Northern China promotes sustainable development of cultivated land. *Agr. Water Manag.* 170, 20–25. <https://doi.org/10.1016/j.agwat.2016.01.009>.
- Zhou, G., Cao, W., Bai, J., Xu, C., Zeng, N., Gao, S., Rees, R.M., Dou, F., 2020. Co-incorporation of rice straw and leguminous green manure can increase soil available nitrogen (N) and reduce carbon and N losses: An incubation study. *Pedosphere* 30, 661–670. [https://doi.org/10.1016/S1002-0160\(19\)60845-3](https://doi.org/10.1016/S1002-0160(19)60845-3).
- Zhou, G., He, Q., Ji, Y., 2016. Advances in the international action and agricultural measurements of adaptation to climate change. *J. Appl. Meteor. Sci.* 27, 527–533. <https://doi.org/10.11898/1001-7313.20160502>.
- Zhou, Z., Wang, M., Feng, X., Qin, J., Wang, A., Ma, H., Chu, G., Liu, Y., Xu, C., Zhang, X., Wang, D., Zheng, X., Chen, S., 2024b. Effects of crop rotation patterns and nitrogen fertilizer levels on storage and structure of soil organic carbon in paddy fields. *Chin. J. Rice Sci.* 1–31. <https://doi.org/10.16819/j.1001-7216.2024.230912>.
- Zhou, N., Zhang, H., Wang, J., Zhang, A., Yang, W., Tang, S., Han, S., Wang, Y., 2024a. Can midseason drainage mitigate methane emissions from a paddy field with milk vetch (*Astragalus sinicus* L.) incorporation? *Soil Till. Res.* 239, 106026. <https://doi.org/10.1016/j.still.2024.106026>.
- Zhu, Z.K., Xiao, M.L., Wei, L., Wang, S., Ding, J.N., Chen, J.P., Ge, T.D., 2022. Key biogeochemical processes of carbon sequestration in paddy soil and its countermeasures for carbon neutrality. *Chin. J. Eco-Agric.* 30, 592–602. <https://doi.org/10.12357/cjea.20210748>.